Miao YW, Feng JQ, Wang JR *et al.* A multi-channel salience based detail exaggeration technique for 3D relief surfaces. JOURNAL OF COMPUTER SCIENCE AND TECHNOLOGY 27(6): 1100– 1109 Nov. 2012. DOI 10.1007/s11390-012-1288-y

A Multi-Channel Salience Based Detail Exaggeration Technique for 3D Relief Surfaces

Yong-Wei Miao[1] (缪永伟), *Senior Member*, *CCF*, Jie-Qing Feng[2] (冯结青), *Senior Member*, *CCF*, Jin-Rong Wang[2] (王金荣), and Renato Pajarola[3]

[1] *College of Computer Science and Technology, Zhejiang University of Technology, Hangzhou 310023, China*

[2] *State Key Lab of CAD & CG, Zhejiang University, Hangzhou 310027, China*

[3] *Department of Informatics, University of Zürich, Zürich CH-8050, Switzerland*

E-mail: ywmiao@zjut.edu.cn; {jqfeng, wangjinrong}@cad.zju.edu.cn; pajarola@ifi.uzh.ch

Received September 4, 2012; revised September 17, 2012.

Abstract Visual saliency can always persuade the viewer's visual attention to fine-scale mesostructure of 3D complex shapes. Owing to the multi-channel salience measure and salience-domain shape modeling technique, a novel visual saliency based shape depiction scheme is presented to exaggerate salient geometric details of the underlying relief surface. Our multi-channel salience measure is calculated by combining three feature maps, i.e., the 0-order feature map of local height distribution, the 1-order feature map of normal difference, and the 2-order feature map of mean curvature variation. The original relief surface is firstly manipulated by a salience-domain enhancement function, and the detail exaggeration surface can then be obtained by adjusting the surface normals of the original surface as the corresponding final normals of the manipulated surface. The advantage of our detail exaggeration technique is that it can adaptively alter the shading of the original shape to reveal visually salient features whilst keeping the desired appearance unimpaired. The experimental results demonstrate that our non-photorealistic shading scheme can enhance the surface mesostructure effectively and thus improving the shape depiction of the relief surfaces.

Keywords multi-channel salience, salience-domain shape modeling, detail exaggeration, shape depiction, relief surface

1 Introduction

Relief surface, one typical 3D highly-detailed complex shape, is composed of two layers of geometry, that is, a smooth low-frequency base surface and a high-frequency geometric detail surface. Here, the high-frequency fine-scale geometric details can be represented as a height function defined on the base surface[1-3], that is, the signed distance from the base surface to the relief surface along the direction of the base's unit normal. These geometric details of 3D complex shapes are usually called in the literature as relief texture or surface mesostructure[4-6], which can guide the viewer's visual attention effectively in the low-level human vision.

Based on the research on the visual depiction of images and 3D shapes[7-13], artists and illustrators usually employ the principles of visual perception for guiding the viewer's attention to visually salient regions. Owing to its efficiency of visual persuasion in traditional art and technical illustrations, visual saliency has now been widely used in the saliency-guided shape enhancement for object visualization[14-16].

In this paper, we propose a novel scheme for bringing out the fine-scale relief details of complex shapes, which can guide the viewer's attention to the surface mesostructure. The main contributions of this paper are as follows.

1) *Multi-Channel Salience Measure.* A definition of multi-channel salience measure for relief surfaces is presented by combining three feature maps, i.e., the 0-order feature map of local height distribution, the 1-order feature map of normal difference, and the 2-order feature map of mean curvature variation.

2) *Salience-Based Detail Exaggeration Operation.* Incorporating the multi-channel salience measure into the salience-domain shape manipulation function, a novel salience-based shape depiction scheme is

Regular Paper

This work was supported by the National Natural Science Foundation of China under Grant Nos. 61272309, 61170138 and the Program for New Century Excellent Talents in University of China under Grant No. NCET-10-0728.

*The preliminary version of the paper was published in the Proceedings of the 2012 Computational Visual Media Conference.

illustrated to exaggerate surface salient geometric details.

3) *Salience-Guided Non-Photorealistic Shading.* Our proposed shape depiction technique can adaptively alter surface shading to enhance surface fine-scale geometric details in a non-photorealistic manner, which is performed by adjusting the surface normals whilst keeping the desired appearance unimpaired.

Compared with the preliminary version of the shape enhancement technique in [17], a detailed computational framework of our multi-channel salience measure is illustrated and our algorithm for the detail exaggeration technique is also elaborated. The effectiveness of our algorithm is demonstrated by the experimental results and comparisons in this paper. The rest of this paper is structured as follows. Section 2 reviews some related work of the detail exaggeration and shape depiction techniques. The computational framework of our multi-channel salience for relief surfaces is described in Section 3. Section 4 illustrates the extraction of relief height field on relief surfaces and our salience-based detail exaggeration technique. Some experimental results and discussions are given in Section 5. Finally, Section 6 concludes the paper and gives some directions for future research.

2 Related Work

For conveying and highlighting the fine-scale mesostructure of 3D relief surfaces, many detail exaggeration techniques have been presented to alter the surface shading and illumination effects based on local surface geometries and lighting attributes.

One type of detail enhancement approach is to adjust the geometric vertex positions to improve the illustration of 3D complex shapes. Displacement mapping[18] is the first technique that represents high-frequency geometric details by adding mesostructure properties to the underlying shapes. The view-dependent displacement mapping proposed by Wang *et al.*[19] can synthesize the real 3D highly-detailed geometry by modeling the surface displacements along the viewing direction. Zhou *et al.*[20] developed a mesh quilting technique to synthesize the geometric details by stitching together the corresponding geometry elements in adjacent mesostructure patches. Building upon the Lee's mesh saliency measure[10], Kim and Varshney[16] developed a technique to alter vertex position information to elicit greater visual attention. However, these vertex-modulation schemes may impair the shape appearance of the underlying model during the geometry modification operation.

Another type of detail exaggeration approach is to enhance the visualization of 3D complex shapes by perturbing the surface normals or altering reflection rules based on local surface information. Early in 1978, Blinn extended the traditional color texture mapping to the bump mapping technique[21], which can generate visual effects of bumps and depressions by disturbing surface normals according to a bump map. The normal perturbation technique proposed by Cignoni *et al.*[22] can enhance the surface features by a simple high-frequency enhancement operation of the surface normals. Their simple normal sharpening scheme is efficient to enhance the shading of regular CAD models but not very suitable to the highly detailed complex shapes. Ritshel *et al.*[23] proposed an unsharp masking technique to increase the contrast of reflected radiance in 3D scenes, and thus enhanced the depiction of various visual cues. Inspired by the principles for cartographic terrain relief, the exaggerated shading of Rusinkiewicz *et al.*[24] locally adjusts the light direction over different areas of the underlying surfaces to depict the surface relief at grazing angles. The light warping technique presented by Vergne *et al.*[25] can enhance surface main features with arbitrary material and illumination attributes by warping the incoming light at each surface point. Furthermore, depending on both surface materials and curvature characteristics, Vergne *et al.*[26] presented a technique called radiance scaling for the shape depiction by adjusting reflected light intensities. Zhang *et al.*[27] proposed an interactive scheme for controllable shape exaggeration by using an adaptive exaggeration function. Based on a feature sensitive metric and the idea of integral invariants, Lai *et al.*[28] developed a robust geometric feature extraction and classification algorithm. Wang *et al.*[29] presented a versatile geometric detail editing approach for 3D meshes by filtering the Laplacian coordinates.

However, all of these techniques pay attention to stylized depiction of 3D shapes but do not consider the impact of visual saliency during the shape depiction. The visual saliency is regarded as an important factor to guide a viewer's visual attention. Here, we would seek the novel non-photorealistic shading technique that can enhance the shape depiction explicitly. Incorporating the multi-channel salience into the detail manipulation operation, a novel saliency-guided shading scheme is presented to exaggerate the geometric details and thus improve the 3D shape depiction for highly-detailed relief surfaces.

3 Multi-Channel Salience Measure of Relief Surfaces

As a classical definition of image saliency, Itti *et al.*[7] calculated the saliency map by applying center-surround filtering to different multi-scale image feature

maps. Inspired by Itti's saliency model, Lee *et al.*[10] presented a computational framework of mesh saliency based on the multi-scale center-surround filters with Gaussian-weighted mean curvatures. However, as a local shape descriptor, the mean curvature measure can only characterize the differential property in an infinitesimal neighborhood of the underlying surface. Cipriano *et al.*[30] provided the multi-scale shape descriptors to capture the shape of a neighborhood around a central vertex by fitting a quadratic surface. Employing the center-surround bilateral filter operator on local projection heights between the vertex and its neighbors, Miao and Feng[31] proposed a perceptual-saliency measure to extract the perceptual-saliency extremum lines for 3D shape illustration.

Here, in order to guide the viewer's attention to the fine-scale surface mesostructure and thus exaggerate the visually salient features, we take the multi-channel salience measure as an input of our non-photorealistic shape depiction algorithm. Different from the previous definitions, our salience definition of relief surfaces is based on the multi-channel scheme. It is the combination of three different bottom-up feature maps, i.e., the 0-order feature map of local height distribution, the 1-order feature map of normal difference, and the 2-order feature map of mean curvature variation.

3.1 Feature Map of Local Height Distribution

Given an original relief surface, its local height distribution can give us 0-order geometric information of the underlying surface variation around the sampled vertex. The varied difference of relief height between each vertex and its neighboring vertices can always attract the viewer's visual attention and then be regarded as a cue to define the visual saliency.

Let $\zeta_k^h(\boldsymbol{v})$ denote the Gaussian-weighted average of the local height, it can be calculated as,

$$\zeta_k^h(\boldsymbol{v}) = \frac{\sum\limits_{\boldsymbol{x}\in N_k(\boldsymbol{v})} \langle \boldsymbol{n_v}, \boldsymbol{v}-\boldsymbol{x}\rangle \exp[-\|\boldsymbol{x}-\boldsymbol{v}\|^2/(2\sigma^2)]}{\sum\limits_{\boldsymbol{x}\in N_k(\boldsymbol{v})} \exp[-\|\boldsymbol{x}-\boldsymbol{v}\|^2/(2\sigma^2)]}, \tag{1}$$

where N_k denotes the k-ring neighbors of vertex $\boldsymbol{v}$, $\boldsymbol{n_v}$ is the normal vector of vertex $\boldsymbol{v}$, σ is the standard deviation of the Gaussian filter and it is set as 1.0 in our practice. The term $\langle \boldsymbol{n_v}, \boldsymbol{v}-\boldsymbol{x}\rangle$ means the inner product between vectors $\boldsymbol{n_v}$ and $\boldsymbol{v}-\boldsymbol{x}$, which reflects the local projection height of its neighbor $\boldsymbol{x}$ on $\boldsymbol{n_v}$. Here, the feature map of local height distribution can be expressed as the absolute difference between the Gaussian-weighted averages of local height computed at fine and coarse scales, that is, $S^h(\boldsymbol{v}) = \|\zeta_2^h(\boldsymbol{v}) - \zeta_1^h(\boldsymbol{v})\|$.

3.2 Feature Map of Normal Difference

Furthermore, surface normals give us the 1-order geometric information of the underlying surface variation around the sampled vertex, and the variation of normal directions can reflect the intrinsic features. A large variation of normal fields always means salient geometric features of underlying models and attracts viewers' visual attention. Thus, the varied difference of normal directions can be regarded as the second cue to define the visual saliency.

Let $\zeta_k^n(\boldsymbol{v})$ denote the Gaussian-weighted average of surface normal difference determined as,

$$\zeta_k^n(\boldsymbol{v}) = \frac{\sum\limits_{\boldsymbol{x}\in N_k(\boldsymbol{v})} \triangle n(\boldsymbol{v},\boldsymbol{x}) \exp[-\|\boldsymbol{x}-\boldsymbol{v}\|^2/(2\sigma^2)]}{\sum\limits_{\boldsymbol{x}\in N_k(\boldsymbol{v})} \exp[-\|\boldsymbol{x}-\boldsymbol{v}\|^2/(2\sigma^2)]}, \tag{2}$$

where N_k denotes the k-ring neighbors of vertex $\boldsymbol{v}$, σ is the standard deviation of the Gaussian filter and it is set as 1.0 in our practice. The term $\triangle n(\boldsymbol{v},\boldsymbol{x})$ means the normal difference between vertex $\boldsymbol{v}$ and its neighboring one $\boldsymbol{x}$. It can be computed as $\triangle n(\boldsymbol{v},\boldsymbol{x}) = \frac{1.0-\langle \boldsymbol{n_v},\boldsymbol{n_x}\rangle}{1.0+\|\boldsymbol{v}-\boldsymbol{x}\|/C}$, where $\boldsymbol{n_x}$ means the normal vector of vertex $\boldsymbol{x}$, the constant C can be chosen as $d/10.0$, and d is the diagonal length of the bounding box for the whole model. Here, the feature map of normal difference can be expressed as the absolute difference between the Gaussian-weighted averages of normal difference computed at fine and coarse scales, that is, $S^n(\boldsymbol{v}) = \|\zeta_2^n(\boldsymbol{v}) - \zeta_1^n(\boldsymbol{v})\|$.

3.3 Feature Map of Mean Curvature Variation

Thirdly, surface curvatures reflect the 2-order geometric information of the underlying surface variation around the sampled vertex. The varied difference of mean curvature between each vertex and its neighboring vertices lead to saliency or non-saliency and it can then be regarded as the third cue to define the visual saliency.

Let $\zeta_k^c(\boldsymbol{v})$ denote the Gaussian-weighted average of the surface mean curvature variation, it can be determined as,

$$\zeta_k^c(\boldsymbol{v}) = \frac{\sum\limits_{\boldsymbol{x}\in N_k(\boldsymbol{v})} (c(\boldsymbol{v}) - c(\boldsymbol{x})) \exp[-\|\boldsymbol{x}-\boldsymbol{v}\|^2/(2\sigma^2)]}{\sum\limits_{\boldsymbol{x}\in N_k(\boldsymbol{v})} \exp[-\|\boldsymbol{x}-\boldsymbol{v}\|^2/(2\sigma^2)]}, \tag{3}$$

where $c(\boldsymbol{v})$ means the mean curvature at vertex $\boldsymbol{v}$ (it is estimated by the Taubin's method[32]), N_k denotes the k-ring neighbors of vertex $\boldsymbol{v}$, σ is the standard deviation of the Gaussian filter and it is set as 1.0 in our practice. Here, the feature map of mean curvature

variation can be expressed as the absolute difference between the Gaussian-weighted averages of curvature variation computed at fine and coarse scales, that is, $S^c(\boldsymbol{v}) = \|\zeta_2^c(\boldsymbol{v}) - \zeta_1^c(\boldsymbol{v})\|$.

3.4 Multi-Channel Salience Map of Relief Surfaces

Finally, similar to the definition of image saliency developed by Itti *et al.*[7], a non-linear suppression operator $\mathfrak{N}(\cdot)$ is adopted to reduce the number of salient points of the above three feature maps before combining them. It can help the user to define what makes something unique, and therefore potentially salient features. For each feature map S^*, we first normalize it to $[0.0, 1.0]$, and then compute the maximum salience value M^* and the average m^* of the local maxima excluding the global maximum. The suppression step $\mathfrak{N}(S^*)$ will multiply S^* by the factor $(M^* - m^*)^2$, i.e.,

$$\mathfrak{N}(S^*)(\boldsymbol{v}) = S^*(\boldsymbol{v}) \cdot (M^* - m^*)^2.$$

The final multi-channel mesh salience $S(\boldsymbol{v})$ can thus be determined by averaging all of the three feature maps after applying the non-linear normalization of suppression[7], that is,

$$S(\boldsymbol{v}) = \frac{1}{3}\mathfrak{N}(S^h)(\boldsymbol{v}) + \frac{1}{3}\mathfrak{N}(S^n)(\boldsymbol{v}) + \frac{1}{3}\mathfrak{N}(S^c)(\boldsymbol{v}).$$

Fig.1 gives our multi-channel salience computation steps for Armadillo model. The final multi-channel salience map (see Fig.1(e)) combines three feature maps, which are in terms of local height distribution (see Fig.1(b)), normal difference (see Fig.1(c)), and mean curvature variation (see Fig.1(d)) respectively. In this paper, the warm colors (red and yellow) always indicate high value, whilst the cool colors (green and blue) always indicate low value of the corresponding field. Fig.2 gives the estimated multi-channel salience maps for Dragon, Armadillo and Pegaso model, respectively. Our multi-channel salience maps can account for illustrating salient geometric details of different relief surfaces.

However, if compared with the traditional mesh saliency map[10] (see Fig.3(b)), our multi-channel salience map of complex shapes (see Fig.3(d)) can reflect

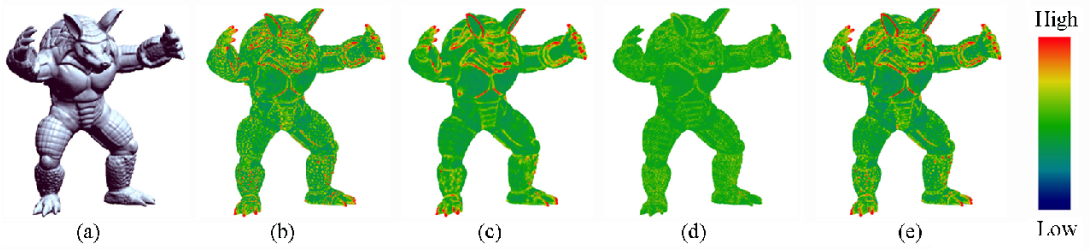

Fig.1. Multi-channel salience computation steps for Armadillo model. (a) Original Armadillo model. (b), (c), (d) Feature maps of local height distribution, normal difference, and mean curvature variation, respectively. (e) Final combined multi-channel salience map.

Fig.2. Multi-channel salience maps for different models. (a) Different original models. (b) Multi-channel salience maps for different models.

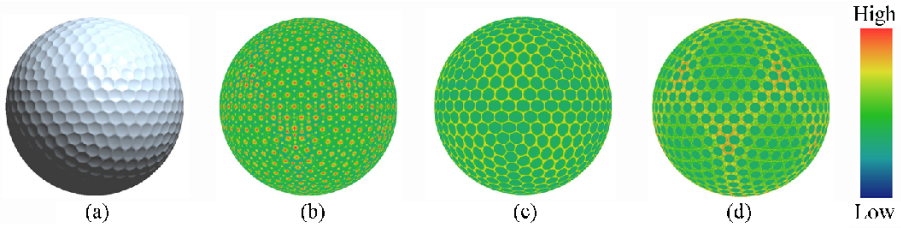

Fig.3. Different mesh saliency definitions for golf ball model. (a) Original golf ball model. (b) Traditional mesh saliency map[10] in terms of multi-scale center-surround Gaussian filtering on mean curvature distribution. (c) Perceptual saliency map[31] in terms of center-surround bilateral filtering on the local projection heights. (d) Our multi-channel salience map for golf ball model.

effectively the high-frequency mesostructure of the underlying surface, such as the inner part and the brim part of each cell of the golf ball, which can attract the viewer's visual attention. However, the perceptual saliency map[31] (see Fig.3(c)) can only reflect some part of salient geometric features because of its approximate estimation of local projection heights, such as only the brim part of each cell of the golf ball.

4 Multi-Channel Salience Based Detail Exaggeration Technique

Now, guided by the multi-channel salience definition of relief surfaces, a novel detail exaggeration technique is proposed to enhance the shape depiction in this section. The original relief surface is firstly decomposed as the low-frequency base surface and the high-frequency detail surface. The detail layer is then manipulated by a special salience-domain enhancement function, and the enhanced surface can finally be obtained by adjusting the surface normals of the original surface as the corresponding final normals of the manipulated surface. The advantage of our detail exaggeration technique is that it can adaptively alter the shading of the original shape to reveal visually salient features whilst keeping the desired appearance unimpaired.

For the sake of describing our algorithms clearly, we introduce some new concepts used in the following text.

• *Original Relief Surface*: the relief surface provided as an input of the algorithm.

• *Base Surface*: the low-frequency component extracted from the original relief surface.

• *Detail Surface*: the high-frequency component extracted from the original relief surface.

• *Manipulated Surface*: the relief surface which has been modified by the user specified shape manipulation function to the original relief surface.

• *Enhanced Surface*: the relief surface returned by the detail exaggeration algorithm, which has the same geometry as the original relief surface but its surface normals are perturbed to highlight the visually salient regions.

4.1 Shape Decomposition of Relief Surfaces

According to Zatzarinni *et al.*'s indirect approach[1] of surface relief extraction, the original relief surface S (always be represented as the triplet $\{V|S = (\boldsymbol{v}_S, \boldsymbol{N}_S); E|S; F|S\}$ of vertices $V|S$, edges $E|S$, and facets $F|S$) is composed of a smooth base surface $B \subset \mathbb{R}^3$ and a height function $h : S \to \mathbb{R}$, that is,

$$S(\boldsymbol{v}) = B(\boldsymbol{v}) + h(\boldsymbol{v})\boldsymbol{N}_B(\boldsymbol{v}), \tag{4}$$

where the height function $h(\boldsymbol{v})$ represents the signed distance from the base surface B to the surface S along the direction of the base's unit normal $\boldsymbol{N}_B(\boldsymbol{v})$.

Instead of trying to reconstruct explicitly the base surface B, the height function $h(\boldsymbol{v})$ of each vertex $\boldsymbol{v}$ will be determined implicitly through the relative height differences of its neighboring vertices along the base surface normals. For calculating these relative height differences, the normals of base surface should be precomputed via a normal smoothing operation. In practice, we employ the adaptive and anisotropic Gaussian mesh filtering scheme to estimate the face normals of base surface proposed by Ohtake *et al.*[33] Here, the vertex normals of base surface can then be calculated as the normalized average of the normals of the incident faces. Furthermore, by using the estimated vertex normals $\{\boldsymbol{N}_B(\boldsymbol{v}_i),\ i = 1, 2, \ldots, n\}$, we can calculate the relative heights of all vertices on the underlying model by energy minimization. That is, for two adjacent vertices $(\boldsymbol{v}_i, \boldsymbol{v}_j) = \boldsymbol{e}_{i,j} \in E$, the height difference $dh(\boldsymbol{e}_{i,j})$ between these two vertices can be calculated as the projection of the edge vector onto the average normals at $\boldsymbol{v}_i$ and $\boldsymbol{v}_j$,

$$dh(\boldsymbol{e}_{i,j}) = (\boldsymbol{v}_i - \boldsymbol{v}_j) \cdot \boldsymbol{N}_B(\boldsymbol{e}_{i,j}), \tag{5}$$

where $\boldsymbol{N}_B(\boldsymbol{e}_{i,j}) = \frac{\boldsymbol{N}_i+\boldsymbol{N}_j}{2} / \| \frac{\boldsymbol{N}_i+\boldsymbol{N}_j}{2} \|$.

The solution to all the surface relief height values $\{h(\boldsymbol{v}_i),\ i = 1, 2, \ldots, n\}$ can be determined by an overly constrained system of $|E|S|$ equations with $|V|S|$ variables,

$$h(\boldsymbol{v}_i) - h(\boldsymbol{v}_j) = dh(\boldsymbol{e}_{i,j}), \quad \text{for } \forall\ \boldsymbol{e}_{i,j} \in E|S.$$

Thus, the relief height values can be estimated by minimizing the following energy functional:

$$\min_{h(\boldsymbol{v}_i), i=1,2,\ldots,n} \sum_{\boldsymbol{e}_{i,j} \in E} [h(\boldsymbol{v}_i) - h(\boldsymbol{v}_j) - dh(\boldsymbol{e}_{i,j})]^2. \tag{6}$$

It can be solved by the conjugate gradient method[34], which is an iterative method that can be applied to multidimensional functional minimization and is optimal in the mean squared error sense.

Now, if taking the estimated relief height distribution of an original surface $S = \{V|S = (\boldsymbol{v}_S, \boldsymbol{N}_S); E|S; F|S\}$ as input, we can easily determine the base surface as $B(\boldsymbol{v}) = S(\boldsymbol{v}) - h(\boldsymbol{v})\boldsymbol{N}_B(\boldsymbol{v})$. The complex models can then be seen as made up of two layers, i.e., the large features (low-frequency base surface $B(\boldsymbol{v})$) defining its overall shape, plus small features (high-frequency detail surface $h(\boldsymbol{v})\boldsymbol{N}_B(\boldsymbol{v})$) accounting for the relief details.

4.2 Salience-Based Detail Manipulation Operation

To facilitate the advanced shape editing and filtering operations for 3D shapes, Eigensatz *et al.*[35] presented a framework of curvature-domain geometry processing, which performs the editing and filtering operations on the principal curvature domain and thus reconstructs the resulting surface to match the desired target curvatures by employing an energy optimization step. Here, for the sake of detail exaggeration, we firstly obtain the manipulated surface by applying the saliency-domain enhancement shape manipulation function to the original relief surface and then exaggerate the relief details of the original surface only by adjusting its surface normal as the corresponding final normal of the manipulated surface.

Inspired by the Gaussian high-pass filtering and enhancement filtering used in traditional image processing tasks[36], our saliency-domain shape manipulation function can be defined as $H_{\text{hp}}(s) = 1 - \exp[-(s - s_0)^2/(2\mu^2)]$, where s_0 means the average of the relief saliency of the whole model, and the parameter μ is the user-defined standard deviation of the Gaussian function (we set $\mu = 0.001$ in all of our experiments). The saliency-domain enhancement shape manipulation function can then be expressed as follows:

$$R(s) = a + bH_{\text{hp}}(s). \tag{7}$$

Here, $H_{\text{hp}}(s)$ is the Gaussian high-pass shape manipulation function. The two manipulation parameters (a, b) can control final detail exaggeration results. Finally, the vertex normal $\boldsymbol{N}_{\text{enhance}}$ of the enhanced surface can be estimated by averaging the face normals incident to each vertex.

According to Subsection 4.1, we decompose the original surface into base layer and detail layer, and incorporate the relief saliency to influence its detail layer in the enhanced models as follows.

$$E(\boldsymbol{v}) = B(\boldsymbol{v}) + R(s(\boldsymbol{v}))h(\boldsymbol{v})\boldsymbol{N}_B(\boldsymbol{v}), \tag{8}$$

where $E(\boldsymbol{v})$ represents the manipulated surface, and $R(s(\boldsymbol{v}))$ is the user specified shape manipulation function defined on the relief saliency domain.

However, to keep the desired appearance unimpaired, it should be emphasized that we will enhance the shape depiction of 3D complex surfaces by adaptively perturbing surface normals. Now, it is easy for us to perturb the original surface normals, that is, by assigning the final normal $\boldsymbol{N}_{\text{enhance}}$ of the above manipulated surface $E(\boldsymbol{v})$ to the corresponding original surface vertex. The final enhanced surface $S' = \{V|S' = (\boldsymbol{v}_S, \boldsymbol{N}_{\text{enhance}}); E|S; F|S\}$ will improve the shape depiction of the original relief surface.

Fig.4 gives our relief detail exaggeration framework for Armadillo model. The multi-channel salience map of Armadillo model is firstly calculated (see Fig.4(b)) and the relief height distribution is also extracted (see Fig.4(c)). The relief detail exaggerated surface (see Fig.4(d)) can then be obtained in a non-photorealistic shading scheme.

5 Experimental Results and Discussion

The proposed detail exaggeration technique has been implemented on a PC with a Pentium IV 3.0 GHz CPU, 1 024 MB memory. In a preprocessing step, the multi-channel salience map and the relief height distribution for the underlying relief surface are extracted. Then, guided by the saliency definition, our detail exaggeration scheme is effective for various 3D complex models. In detail, for the saliency-driven detail manipulation operation, it will take about 0.35 to 0.88 seconds for various meshes ranging from 72 K to 173 K vertices.

5.1 Different Controls of Detail Exaggeration Results

In our saliency-driven detail exaggeration scheme,

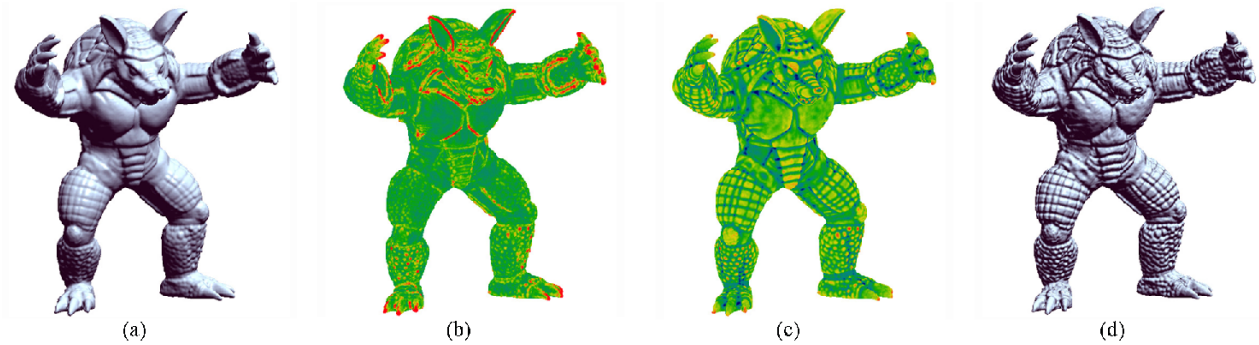

Fig.4. Relief detail exaggeration framework. (a) Original Armadillo model. (b) Multi-channel salience map of Armadillo model. (c) Extracted relief height distribution of Armadillo model. (d) Relief detail exaggeration results for Armadillo using manipulation parameters $(a, b) = (3.0, 2.0)$.

the two manipulation parameters (a, b) introduced in the saliency-domain shape manipulation function $R(s) = a + bH_{\text{hp}}(s)$ will always effect the final detail exaggeration results. Fig.5 shows some detail exaggeration results for Dragon, Armadillo and Pegaso model using different manipulation parameters (a, b) respectively, in which the relief details have been exaggerated whilst keeping the desired appearance unimpaired. Here, the large parameters a and b will bring out more fine-scale salient geometric details of the underlying shape and can convey both detail and overall shape as clearly as possible.

5.2 Comparisons with Different Detail Exaggeration Techniques

Essentially, our proposed visual saliency based detail exaggeration scheme is to improve shape depiction of 3D complex shapes by dynamically perturbing relief surface normals. It is an indirect manner, that is, to enhance the detail layer by employing a saliency-domain shape manipulation function and then improve the surface normals by assigning the normal of the manipulated surface to the corresponding original surface vertex.

One work closely related to our saliency-based shading method is the normal sharpening technique proposed by Cignoni *et al.*[22], which performs the conventional diffuse shading using a sharpened normal field, that is, $\boldsymbol{N}_E = \boldsymbol{N} + k \cdot (\boldsymbol{N} - \boldsymbol{N}_L)$. It depends mainly on two parameters — the value of the weighting constant k and the amount of low-pass filter to generate the smooth normals $\boldsymbol{N}_L$ by iteratively average each face normal with the normals of its adjacent faces. Fig.6 shows some comparisons with different normal perturbation techniques. In the implementation of our saliency-guided detail exaggeration technique, we use the manipulation parameters $(a, b) = (3.0, 2.0)$ for detail manipulation operation (see Fig.6(b)). We also give the salience guided linear normal enhancement result[37] by using our multi-channel salience measure (see Fig.6(d)). Meanwhile, in the implementation of the normal sharpening technique, we choose the weighting constant k as 0.5, which affects the intensity of the normal enhancement effect and takes 10 iterations for normal averaging to smooth the surface normals (see Fig.6(c)). Compared with the simple normal sharpening scheme[22], our multi-channel salience based detail

Fig.5. Relief detail exaggeration results for Dragon, Armadillo and Pegaso model using different manipulation parameters. (a) Original models. Different detail exaggeration results using two manipulation parameters (a, b): (b) $(1.0, 2.0)$. (c) $(3.0, 2.0)$. (d) $(3.0, 4.0)$.

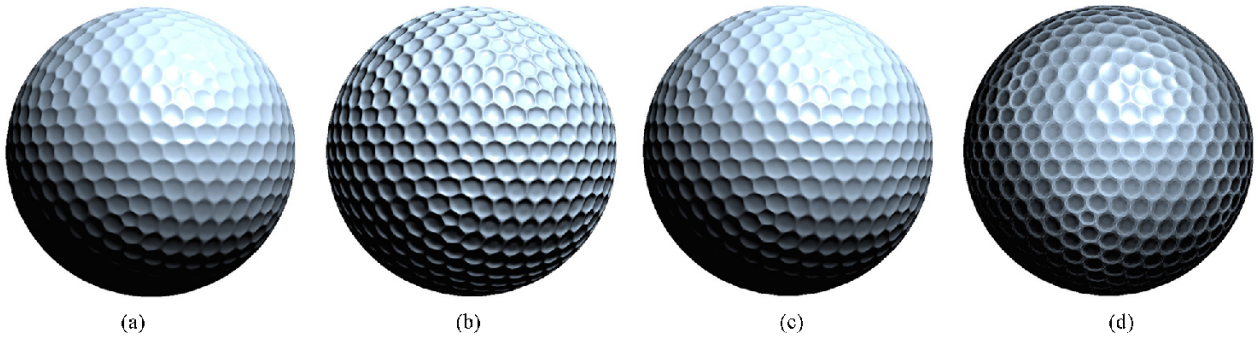

Fig.6. Detail exaggeration results by different normal perturbation techniques for golf ball model. (a) Original golf ball model. (b) Detail exaggeration result by our multi-channel salience based technique using manipulation parameters $(a, b) = (3.0, 2.0)$. (c) Detail exaggeration result by the simple normal sharpening technique[22]. (d) Detail exaggeration result by the linear normal enhancement technique[37] using our multi-channel salience measure.

exaggeration scheme can effectively bring out the fine-scale geometric details of the underlying shape and enhance the visually salient features of the highly-detailed relief surface.

Moreover, compared with other detail exaggeration techniques, our approaches may exaggerate the relief details of the underlying complex shape effectively (See Fig.7). Compared to the exaggerated shading scheme[24], our multi-channel salience based technique can reveal visually salient features without impairing the desired appearance. Compared with the light warping technique[25] and radiance scaling technique[26], our system incorporates the visual salience measure of a polygon mesh into the detail manipulation which can guide viewers' visual attention adequately for expressive rendering.

6 Conclusions and Future Work

In this paper, a multi-channel salience definition for relief surface is presented by combining three feature maps, which are determined in terms of local height distribution, normal difference, and mean curvature variation between each vertex and its neighbors. By incorporating our multi-channel salience measure into the detail exaggeration operation, we develop a novel saliency-guided shape depiction scheme for exaggerating the fine-scale relief details by perturbing the surface normals. The advantage of our approach is that they can effectively enhance the shape depiction by conveying visually salient mesostructure of the relief surfaces. The experimental results demonstrate that our non-photorealistic shading schemes can bring out the surface fine details effectively without impairing the shape appearance.

In the future work, we will introduce some surface enhancement techniques to adjust the lighting component during 3D shape depiction. Meanwhile, we have considered the role of surface salience measure in the context of 3D shape depiction. It will also be interesting to see how other modeling and rendering tasks can benefit from our multi-channel salience measure, such as saliency-guided lighting, saliency-based re-sampling/simplification, and saliency-driven shape modeling.

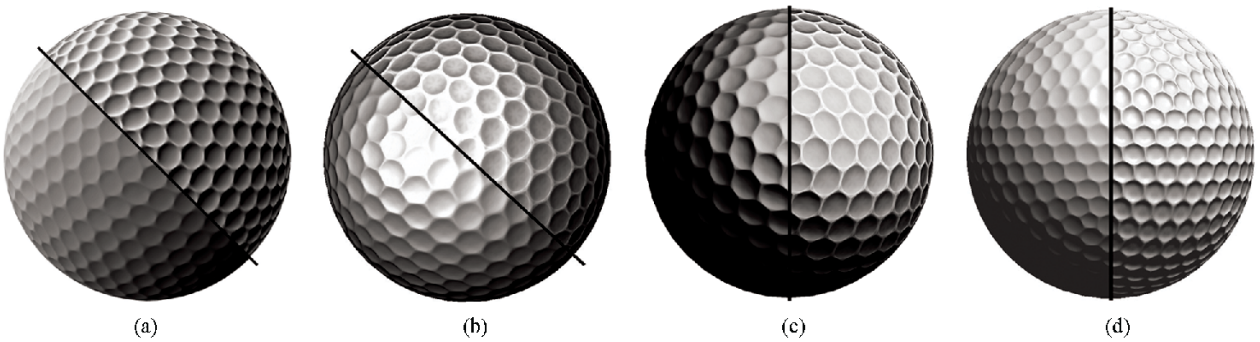

Fig.7. Detail exaggeration comparisons with different surface enhancement techniques for golf ball model. The images of previous techniques are extracted from their corresponding original papers and supplemental materials. (a) Exaggerate shading[24]. (b) Light warping[25]. (c) Radiance scaling[26]. (d) Our multi-channel salience based detail exaggeration technique using manipulation parameters $(a, b) = (3.0, 2.0)$ and white light source.

Acknowledgements The authors would like to thank Prof. Amitabh Varshney for discussions and the anonymous reviewers for their valuable suggestions for improving this paper. The 3D models are courtesy of the Aim@Shape Shape Repository, Rutgers University, Princeton University and Stanford University.

References

[1] Zatzarinni R, Tal A, Shamir A. Relief analysis and extraction. *ACM Transactions on Graphics*, 2009, 28(5), Article No.136.

[2] Kolomenkin M, Shimshoni I, Tal A. On edge detection on surfaces. In *Proc. CVPR*, June 2009, pp.2767-2774.

[3] Kolomenkin M, Shimshoni I, Tal A. Prominent field for shape processing and analysis of archaeological artifacts. *International Journal of Computer Vision*, 2011, 94(1): 89-100.

[4] Dischler J M, Ghazanfarpour D. A procedural description of geometric textures by spectral and spatial analysis of profiles. *Computer Graphics Forum*, 1997, 16(3): 129-139.

[5] Wang J, Dana K J. Relief texture from specularities. *IEEE Transactions on Pattern Analysis and Machine Intelligence*, 2006, 28(3): 446-457.

[6] De Toledo R, Wang B, Levy B. Geometry textures and applications. *Computer Graphics Forum*, 2008, 27(8): 2053-2065.

[7] Itti L, Koch C, Niebur E. A model of saliency based visual attention for rapid scene analysis. *IEEE Transactions on Pattern Analysis and Machine Intelligence*, 1998, 20(11): 1254-1259.

[8] Tood J T. The visual perception of 3D shape. *Trends in Cognitive Sciences*, 2004, 8(3): 115-121.

[9] Agrawala M, Durand F. Guest editors' Introduction: Smart depiction for visual communication. *IEEE Computer Graphics and Applications*, 2005, 25(3): 20-21.

[10] Lee C, Varshney A, Jacobs D. Mesh saliency. *ACM Transactions on Graphics*, 2005, 24(3): 659-666.

[11] Cheng M, Zhang G, Mitra N J, Huang X, Hu S. Global contrast based salient region detection. In *Proc. the 24th CVPR*, June 2011, pp.409-416.

[12] Wang D, Li G, Jia W, Luo X. Saliency-driven scaling optimization for image retargeting. *The Visual Computer*, 2011, 27(9): 853-860.

[13] Lee H, Lavoué G, Dupont F. Rate-distortion optimization for progressive compression of 3D mesh with color attributes. *The Visual Computer*, 2012, 28(2): 137-153.

[14] Viola I, Feixas M, Sbert M, Gröller M. Importance-driven focus of attention. *IEEE Transactions on Visualization and Computer Graphics*, 2006, 12(5): 933-940.

[15] Kim Y, Varshney A. Saliency-guided enhancement for volume visualization. *IEEE Transactions on Visualization and Computer Graphics*, 2006, 12(5): 925-932.

[16] Kim Y, Varshney A. Persuading visual attention through geometry. *IEEE Transactions on Visualization and Computer Graphics*, 2008, 14(4): 772-782.

[17] Miao Y, Feng J, Wang J, Pajarola R. A shape enhancement technique based on multi-channel salience measure. In *Lecture Notes in Computer Science 7633*, Hu S M, Martin R R (eds.), 2012, pp.115-121.

[18] Cook R L. Shade trees. *Computer Graphics*, 1984, 18(3): 223-231.

[19] Wang L, Wang X, Tong X, Lin S, Hu S, Guo B, Shum H Y. View-dependent displacement mapping. *ACM Transactions on Graphics*, 2003, 22(3): 334-339.

[20] Zhou K, Huang X, Wang X, Tong Y, Desbrun M, Guo B, Shum H Y. Mesh quilting for geometric texture synthesis. *ACM Transactions on Graphics*, 2006, 25(3): 690-697.

[21] Blinn J F. Simulation of wrinkled surfaces. *Computer Graphics*, 1978, 12(3): 286-292.

[22] Cignoni P, Scopigno R, Tarini M. A simple normal enhancement technique for interactive non-photorealistic renderings. *Computers & Graphics*, 2005, 29(1): 125-133.

[23] Ritschel T, Smith K, Ihrke M, Grosch T, Myszkowski K, Seidel H P. 3D unsharp masking for scene coherent enhancement. *ACM Transactions on Graphics*, 2008, 27(3), Article No. 90.

[24] Rusinkiewicz S, Burns M, DeCarlo D. Exaggerated shading for depicting shape and detail. *ACM Transactions on Graphics*, 2006, 25(3): 1199-1205.

[25] Vergne R, Pacanowski R, Barla P, Granier X, Schlick C. Light warping for enhanced surface depiction. *ACM Transactions on Graphics*, 2009, 28(3), Article No. 25.

[26] Vergne R, Pacanowski R, Barla P, Granier X, Schlick C. Radiance scaling for versatile surface enhancement. In *Proc. Symposium on Interactive 3D Graphics and Games*, Feb. 2010, pp.143-150.

[27] Zhang X, Chen W, Fang J, Wang R, Peng Q. Perceptually-motivated shape exaggeration. *The Visual Computer*, 2010, 26(6-8): 985-995.

[28] Lai Y, Zhou Q, Hu S, Wallner J, Pottmann H. Robust feature classification and editing. *IEEE Transactions on Visualization and Computer Graphics*, 2007, 13(1): 34-45.

[29] Wang H, Chen H, Su Z, Cao J, Liu F, Shi X. Versatile surface detail editing via Laplacian coordinates. *The Visual Computer*, 2011, 27(5): 401-411.

[30] Cipriano G, Phillips G N, Gleicher M. Multi-scale surface descriptors. *IEEE Transactions on Visualization and Computer Graphics*, 2009, 15(6): 1201-1208.

[31] Miao Y, Feng J. Perceptual-saliency extremum lines for 3D shape illustration. *The Visual Computer*, 2010, 26(6-8): 433-443.

[32] Taubin G. Estimating the tensor of curvature of a surface from a polyhedral approximation. In *Proc. the 5th ICCV*, June 1995, pp.902-907.

[33] Ohtake Y, Belyaev A, Seidel H P. Mesh smoothing by adaptive and anisotropic Gaussian filter applied to mesh normals. In *Proc. Vision, Modeling and Visualization*, Nov. 2002, pp.203-210.

[34] Press W H, Flannery B P, Teukolsky S A, Vetterling W T. Numerical Recipes in C: The Art of Scientific Computing (2nd edition). New York, USA: Cambridge University Press, 1992.

[35] Eigensatz M, Sumner R W, Pauly M. Curvature-domain shape processing. *Computer Graphics Forum*, 2008, 27(2): 241-250.

[36] Gonzalez R C, Woods R E. Digital Image Processing (2nd edition). New Jersey, USA: Prentice Hall, 2002.

[37] Miao Y, Feng J, Pajarola R. Visual saliency guided normal enhancement technique for 3D shape depiction. *Computers & Graphics*, 2011, 35(3): 706-712.

Yong-Wei Miao received his M.Sc degree in differential geometry from the Chinese Academy of Sciences in 1996 and his Ph.D. degree in computer graphics from the State Key Lab of CAD & CG at Zhejiang University in 2007. He is a professor in Zhejiang University of Technology, China. His research interests include digital geometry processing, computer vision, and computer-aided geometric design.

Jie-Qing Feng received his B.Sc. degree in applied mathematics from the National University of Defense Technology in 1992 and his Ph.D. degree in computer graphics from Zhejiang University in 1997. He is a professor in the State Key Lab of CAD & CG, Zhejiang University, China. His research interests include geometric modeling, real-time rendering and computer animation.

Jin-Rong Wang received his M.Sc degree in cryptography theory and practice from Hangzhou Dianzi University in 2004. He is currently a Ph.D. candidate in the State Key Lab of CAD & CG, Zhejiang University, China. His research interests include digital geometry processing, digital watermarking, and information security.

Renato Pajarola received his Dr. Sc. Techn. degree in computer science from the Swiss Federal Institute of Technology (ETH) Zürich in 1998. After a postdoc at Georgia Tech., he joined the University of California Irvine in 1999 as an assistant professor. He is an associate professor in University of Zürich, Switzerland. His research interests include real-time 3D graphics, scientific visualization, and interactive 3D multimedia.